Alessandra C. Pinheiro, Thaís C. M. Nogueira, Cristiane França da Costa, Cristina Lourenço, John N. Low, James L. Wardell*, Solange M. S. V. Wardell and Marcus V. N. de Souza

A study of antituberculosis activities and crystal structures of (*E*)-2-[2-(arylidene)hydrazinyl] pyrimidine and (*E*)-N^1-(arylidene)pyrimidine-2-carbohydrazide derivatives

https://doi.org/10.1515/znb-2020-0108
Received June 10, 2020; accepted October 20, 2020; published online November 24, 2020

Abstract: A study of the anti-tuberculosis activity against *Mycobacterium tuberculosis* ATTC 27294 and an X-ray structural determination of (*E*)-2-[2-(arylidene)hydrazinyl]pyrimidine, **1**, and (*E*)-N^1-(arylidene)pyrimidine-2-carbohydazide, **2**, derivatives are presented. The effect of the substituents in the aryl moiety on the antituberculosis (anti-TB) activities of **1** and **2** is compared with that of other heteroaryl hydrazonyl and acylhydrazonyl derivatives. The biological activities of **1** do not depend on the coordinating ability of the substituted aryl group: in **2**, the most effective aryl group is 5-nitrofuranyl. The structure determinations of (*E*)-2-((2-(pyrimidin-2-yl)hydrazono)methyl)-phenol, (*E*)-*N*′-(2,5-dihydroxybenzylidene)pyrimidine-2-carbohydrazide and of the hydrate of (*E*)-*N*′-(2-hydroxy-4-methylbenzylidene) pyrimidine-2-carbohydrazide, and a literature search of related structures in the CCDC data base, allowed an examination of the more important interactions, including the occurrence of X–Y···π interactions.

Keywords: anti-TB; (*E*)-2-[2-(arylidene)hydrazinyl]pyrimidines; (*E*)-N^1-(arylidene)pyrimidine-2-carbohydazides; X-ray crystallography; π interactions.

***Corresponding author: James L. Wardell,** Fundação Oswaldo Cruz, Instituto de Tecnologia em Fármacos - Farmanguinhos, 21041-250, Rio de Janeiro, RJ, Brazil; and Department of Chemistry, University of Aberdeen, Meston Walk, Old Aberdeen, AB24 3UE, Scotland, UK, E-mail: j.wardell@abdn.ac.uk
Alessandra C. Pinheiro, Thaís C. M. Nogueira, Cristiane França da Costa and Marcus V. N. de Souza, Fundação Oswaldo Cruz, Instituto de Tecnologia em Fármacos - Farmanguinhos, 21041-250, Rio de Janeiro, RJ, Brazil
Cristina Lourenço, Departamento de Bacteriologia, Fundação Oswaldo Cruz, Instituto Nacional de Infectologia Evandro Chagas, 21045-900, Manguinhos, Rio de Janeiro, Brazil
John N. Low, Department of Chemistry, University of Aberdeen, Meston Walk, Old Aberdeen, AB24 3UE, Scotland, UK
Solange M. S. V. Wardell, CHEMSOL, 1 Harcourt Road, Aberdeen AB15 5NY, Scotland, UK

1 Introduction

The pyrimidine moiety (Figure 1) is found in many compounds associated with a wide spectrum of biological activities [1, 2], including antineoplastic [3–6], antibacterial [7, 8], antimalarial [9], antiviral [10] and anti-inflammatory [11], antimicrobial and anti-oxidant [12], leishmanial [13, 14] agents. The potential of arylhydrazone derivatives, especially of nitrogen heteroaromatics, as biological agents has been extensively studied [15–18]. Over the recent past, the de Souza group has investigated the biological activity of a series of such compounds, including anticancer [19–23], antiparasitic [24], antileishmanial [25–27] and anti-tuberculosis (TB) agents [28–35]. The crystal structures of such compounds have also attracted our interest [20, 21, 36–41].

Compounds combining the pyrimidin-2-yl moiety and the hydrazonyl functionality have not been excluded from the general interest in arylhydrazone derivatives, and such compounds have been involved in studies on docking with enzymes [42], antimicrobial activity [43, 44], anticancer [45, 46] and antileishmanial agents [25–27].

Some of us recently reported on the anti-leishmanial activity of a series of hydrazone andacylhydrazone derivatives, built from pyrimidin-2-ylhydrazine and 2-pyridinoic acid, respectively [25]. In continuation of our biological activity studies of nitrogen-containing heteroarene hydrazones and acylhydrazones, we have tested the pyrimidin-2-yl-hydrazone and -acylhydrazone derivatives in an anti-TB study (Scheme 1).

Tuberculosis is a mycobacterial infection, transmitted through the air and mainly affecting the lungs. It has been considered a global health emergency by the World Health Organization (WHO) due to the advent of multidrug-resistant tuberculosis (MDR-TB) and extensively drug-resistant

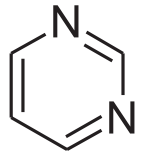

pyrimidine

Figure 1: Chemical structure of pyrimidine.

tuberculosis (XDR-TB) strains. Multidrug-resistant tuberculosis (MDR-TB) refers to organisms that are resistant to the first-line drugs isoniazid and rifampin, and is responsible for about 3.3% of all new cases every year. Extensively drug-resistant tuberculosis (XDR-TB), confirmed in more than 58 countries, is resistant to main first and second line anti-TB drugs and is the biggest challenge in the treatment of this disease [47, 48].

We now wish to report on our findings of the anti-TB activities of a series of pyrimidin-2-yl-hydrazone, **1**, and -acylhydrazone, **2**, derivatives (Scheme 1), and compare the activities with those found in earlier studies of other heteroaryl-hydrazone, and -acylhydrazone, derivatives. We also report on the crystal structures of three derivatives used in this study, namely (*E*)-2-((2-(pyrimidin-2-yl)hydrazono)methyl)phenol (**1a**), (*E*)-*N*′-(2,5-dihydroxybenzylidene) pyrimidine-2-carbohydrazide (**2d**) and the hydrate of **2e**, (*E*)-*N*′-(2-hydroxy-4-methylbenzylidene)pyrimidine-2-carbohydrazide, **2e·(H$_2$O)**. A search of the CCDC data base on 29th April 2020 [49] indicated that very few structures of pyrimidin-2-yl-hydrazones and -acylhydrazones have been reported, certainly in comparison to other nitrogen-containing heteroaryl-NH–N=CH-aryl and -heteroaryl-CO–NH–N=CH-aryl compounds: indeed for the substructure {2–(C—C=N–NH)-pyrimidine} only 13 hits were found. The only structures of the pyrimidin-2-yl-acylhydrazone derivatives that have been reported are the two discussed in this article.

2 Experimental

2.1 General

The pyrimidin-2-ylhydrazone and -acylhydrazone derivatives were prepared as previously reported (Scheme 1). All compounds had m.p.s, NMR and IR spectra and mass spectrometric data as previously reported [25].

2.2 Anti-mycobacterial activity

The anti-mycobacterial activities of compounds **1** and **2** were assessed against *Mycobacterium tuberculosis* ATTC 27294 using the micro plate Alamar Blue assay (MABA) [50]. This methodology is nontoxic, uses a thermally stable reagent and shows good correlation with proportional and BACTEC radiometric methods [51, 52]. The method is described as follows: sterile deionized water (200 mL) was added to all outer-perimeter wells of 96 sterile well plates (Falcon, 3072: Becton Dickin). Each of the 96 plates received 100 mL of Middlebrook 7H9 broth (Difco laboratories, Detroit, MI, USA) and successive dilutions of the tested compound were added directly to the plate. The final drug concentrations tested were 0.01–20.0 mg mL^{-1}. Plates were covered and sealed with parafilm and incubated at T = 37 °C for five days. A freshly prepared 1:1 mixture of Alamar Blue (Accumed International, Westlake, Ohio) reagent and 10% tween 80 (total volume: 25 mL) was added to the plate and incubated for 24 h. A blue colouration in the well was

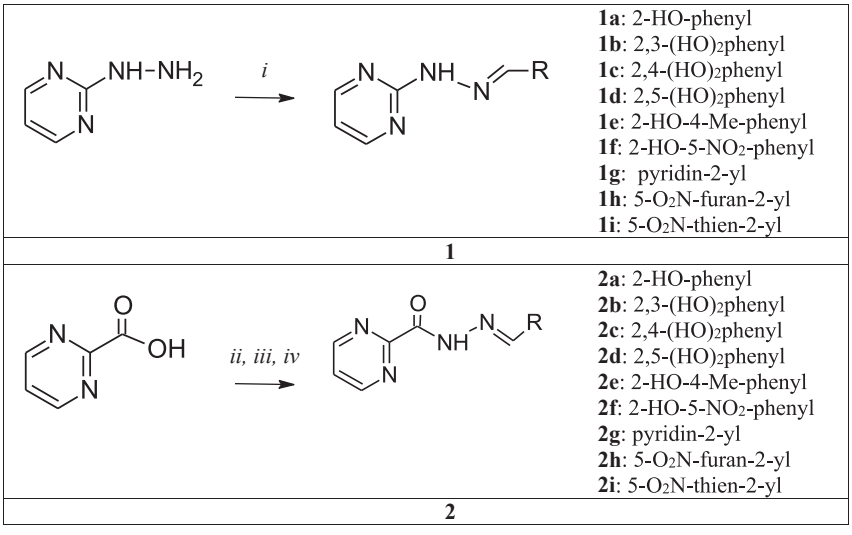

Scheme 1: Reagents: *i*: RCHO, 25 °C; *ii* MeOH, SO_2Cl_2, 25 °C, 24 h; *iii*: $H_2NNH_2 \cdot H_2O$ (80%), EtOH, 25 °C, 3 h; *iv*: RCHO, 25 °C, 1–24 h.

interpreted as no bacterial growth, and a pink colouration was scored as growth. The minimal inhibition concentration (MIC) was defined as the lowest drug concentration, which prevented a colour change from blue to pink.

2.3 Experimental crystallography

Data for compounds was obtained with Mo radiation (λ = 0.71073 Å) at T = 100 K at the NRC crystallographic service, based at the University of Southampton. Data collection, data reduction and unit cell refinement were achieved with CrysAlisPro 1.171.39.9 g [53]. Correction for absorption was achieved by CrysAlisPro 1.171.39.9 g [53]. An empirical absorption correction using spherical harmonics, implemented in the SCALE3 ABSPACK scaling algorithm, was applied. The structures were solved by Direct Methods using Shelxs-97 [54] and fully refined by means of the program Shelxl-97 [54]. The hydroxy hydrogen atom, the hydrogen attached to N3 and the two hydrogens of the water molecule were placed in calculated positions, but then fully refined. All other hydrogen atoms were placed in calculated positions. Shelxl-97 [54] and Platon [55] were used in the calculation of the molecular geometries. The programs Ortep-3 for Windows [56] and Mercury [57] were used in the preparation of the Figures. Crystallographic details are listed in Table 1.

3 Results and discussion

3.1 General

All the compounds were recrystallised samples, prepared as published [25], and were found to have identical ^{1}H and ^{13}C NMR and IR spectra and mass spectrometric data as

Table 1: Crystallographic data.

Compound	1a	2d	2e·(H_2O)
Empirical formula	$C_{11}H_{10}N_4O$	$C_{12}H_{10}N_4O_3$	$C_{13}H_{15}N_4O_3$
Formula weight	214.23	260.23	275.29
Temperature, K	100(2)	100(2)	293(2)
Wavelength λ, Å	0.71073	0.71073	0.71075
Crystal system	monoclinic	monoclinic	monoclinic
Space group	$P2_1/n$	$P2_1/c$	$P2_1/n$
Unit cell dimensions			
a, Å	8.76810(14)	5.6215(6)	4.6855(2)
b, Å	6.41100(10)	29.395(2)	11.6554(4)
c, Å	18.248(3)	6.8344(8)	23.5091(11)
β, deg	99.2300(18)	101.499(12)	93.607(4)
Volume, Å^3	1012.46(17)	1106.7(2)	1281.32(9)
Z	4	4	4
Density (calcd.), Mg m^{-3}	1.41	1.56	1.43
Crystal size, mm^3	0.200 × 0.200 × 0.100	0.070 × 0.060 × 0.015	0.080 × 0.010 × 0.010
Absorption coeff., mm^{-1}	0.1	0.1	0.1
F(000), e	448	540	580
θ Range data coll., deg	2.770–27.484	2.772–27.482	2.463–27.483
Index ranges	$-11 \le h \le 11$	$-7 \le h \le 7$	$-4 \le h \le 6$
	$-8 \le k \le 8$	$-37 \le k \le 34$	$-15 \le k \le 15$
	$-23 \le l \le 23$	$-8 \le l \le 5$	$-29 \le l \le 30$
Reflections collected	11917	8361	16814
Reflections unique	2317	2522	2928
R_{int}	0.0279	0.1159	0.0586
Completeness, %	99.8	100.0	99.9
Absorption correction		Semi-empirical from equivalents	
Transm. max./min.	1.00/0.75	1.00/0.18	1.00/0.88
Refinement method		Full-matrix least-squares on F^2	
Data/parameters	2317/151	2522/181	2928/194
Goodness-of-fit (F^2)	1.037	1.026	0.922
Final R_1/wR_2 [$I > 2\,\sigma(I)$]	0.040/0.105	0.094/0.194	0.045/0.104
Final R_1/wR_2 (all data)	0.042/0.106	0.1865/0.2394	0.071/0.117
Extinction coefficient	n/a	n/a	n/a
Largest diff. peak/hole, e Å^{-3}	0.30/−0.19	0.44/−0.44	0.28/−0.23
CCDC No.	2008878	2008885	2008879

previously reported. The samples of compounds **1a**, **2d** and **2e** used in the X-ray crystallographic study were all further recrystallized from the same batch of methanol.

3.2 Anti-mycobacterial activity

The anti-mycobacterial in-vitro activities of compounds **1** and **2** were tested against *M. tuberculosis* H37Rv strain (ATCC 27294) (Table 2). The biological results, expressed as MIC (μM), for compounds **1** and **2** are listed in Table 2, along with data on the mutagenicity/tumorigenicity and *c* log *P* values. Also listed are the results of using the standard drugs ethambutol and isonicotinic acid hydrazide.

3.2.1 Hydrazone study

In the hydrazone study, the 2-hydroxyphenyl derivatives **1a**–**1f** exhibited a significant range of activities from the most reactive **1f** with a MIC value of 12 μM to significant reactivities of **1b** and **1c**, [MIC ca. 100 μm], and to the unreactive compound **1e** [MIC > 500 μm]. **1f** showed a slightly increased activity over that of ethambutol. The higher reactivity of **1f**, compared to the other 2-hydroxyl substituted compounds, is of interest as a significant role of hydrazones in many biological studies is considered to be that of a di- or poly-dentate chelator, and thereby a potential remover of vital metals from participating in the development of the disease. With its electron withdrawing nitro group, **1f** has a reduced chelating ability than any of the other 2-hydroxyphenyl derivatives used in the study. There is evidence that hydrazones built from heteroarylhydrazines and aldehydes, with suitably *o*-sited donor groups, such as salicylaldehyde and pyridine-2-carbaldehyde derivatives, are effective chelating agents for metals [34, 58, 59]: for metal complexes formed from tridentate hydrazones derived from pyramidin-2-ylhydrazine see references [45, 60–65]. The conclusion that the ability of these pyrimidyl hydrazones is not based solely on their chelating potential is confirmed by the poor activity of the pyridin-2-yl substituent **1g**.

The heteroaryl derivative 2-(2-((5-nitrofuran-2-yl) methylene)hydrazonyl)pyrimidine), **1**h, exhibited a low activity [MIC = 429 μm], while the other heteroaryl derivative 2-(2-((5-nitrothien-2-yl)methylene)hydrazonyl)pyrimidine) (**11)** was non-active. However, hydrazones derived from 5-nitrofuran-2-yl and thieny-2-yl carbaldehydes have shown good activities in other anti-TB studies, e.g., in the study of 7-chloro-4-quinolinylhydrazone derivatives against *M. tuberculosis* H37Rv [30]. Specific nitro-substituted five-membered ring heteroaromatics, in particular MEGAZOL, 5-(1-methyl-5-nitroimidazol-2-yl)-1,3,4-thiadiazol-2-amine) [66] and BENZNIDAZOLE, *N*-benzyl-2-(2-nitroimidazol-1-yl)acetamide [67, 68] have shown good activities as antiparasitic agents. The mechanism of action of these compounds is based on their ready reduction to radical intermediates using a flavine-based enzyme, present in the intracellular media. A radical-based mechanism could also apply with these anti-TB active nitro-heteroaryl compounds. That the 5-nitro-2-hydroxyphenyl derivative **1f** possesses the best activity of all the 2-hydroxyphenyl derivatives studied here could also be related to redox potentials [35].

As mentioned earlier, the same set of pyrimidin-2-ylhydrazones was used in the recent study against promastigotes and Leishmania amazonensis-GFP amastigotes, as well as murine macrophages [25]. Here the compound with the best response was the pyridin-2-yl derivative; indeed most of the compounds studied had good activities. This clearly suggests that a different

Table 2: The in-vitro activity of compounds **1** and **2** against *Mycobacterium tuberculosis* H37Rv strain (ATCC 27294, susceptible to ethambutol).

Compound	Aryl group	MIC (μM)[a]	Mutagenic/ tumorigenic	*c* log *P*[b]
(a) Hydrazones				
1a	2-HO-phenylOH	234	None/none	3.302
1b	2,3-$(HO)_2$-phenyl	109	High/none	2.956
1c	2,4-$(HO)_2$phenyl	109	None/none	2.956
1d	2,5-$(HO)_2$-phenyl	435	None/none	2.956
1e	2-HO- 4-Me-phenyl	>500	None/none	3.645
1f	2-HO-5-O_2N-phenyl	12	None/none	2.380
1g	Pyridin-2-yl	>500	Low/none	2.700
1h	5-O_2N-furan-2-yl	429	High/high	2.266
1i	5-O_2N-thien-2-yl	>500	None/none	2.782
EMB[c]	–	15.3	–	
INH[d]	–	0.46	–	
Compound	**Aryl group**	**MIC (μM)**	**Mutagenic/ tumorigenic**	***c* log *P*[a]**
(b) Acylhydrazones				
2a	2-HO-phenylH	>500	None/none	1.182
2b	2,3-$(HO)_2$-phenyl	>500	High/none	0.837
2c	2,4-$(HO)_2$.phenyl	>500	None/none	0.837
2d	2,5-$(HO)_2$-phenyl	>500	None/none	0.837
2e	2-HO- 4-Me-phenyl	391	None/none	1.526
2f	2-HO-5-O_2N-phenyl	174	None/none	0.261
2g	pyridine-2-yl	>500	Low/none	0.581
2h	5-O_2N-furan-2-yl	48	High/high	0.146
2i	5-O_2N-thien-2-yl	45	None/none	0.103

[a]The minimal inhibition concentration (MIC), which prevented the colour change from blue to pink, [b]Calculated using Data Warrior program [70], [c]EMB = ethambutol, and [d]INH = isonicotinic acid hydrazide.

mechanism applies here, compared to that in the anti-TB situation.

3.2.2 Acylhydrazone study

The most active acylhydrazones studied were **2h** and **2i**. The pyridine-2-yl, **2g**, and the 2-hydroxyphenyl derivatives, **2a**–**2f**, were at best moderately active, so again here a chelating role for the compounds seems not to have a major impact.

The same general reactivity sequence of substituents as found in the current study was reported in a larger study against *M. tuberculosis* H37Rv involving 2-(aryl-CH=N–NHCOCH$_2$)-thienes, having phenyl or heteroaryl moieties [69]: here the most active compounds were the 5-nitrothien-2-yl and 5-nitrofuran-2-yl derivatives, with MIC values of 8.5 and 9.0 μm, respectively. Moderately active compounds were the pyridin-2-yl, and 2- and 4-hydroxyphenyl derivatives, with MIC values between 170 and 408 μm, while the compounds were phenyl derivatives with MeO, F, Cl, Br, CN, and O_2N substituents and the heteroaryl compounds (furan-2-yl, thien-2-yl, pyrrol-2-yl, imidazol-2-yl, pyridin-3-yl, and pyridin-4-yl) were inactive [69]. In a further study using 2-(heteroaryl)-CH=N–NHCO) pyrazine derivatives, the 5-nitrofuran-2-yl derivative was found to be the most active compound (and non-cytotoxic) [29] among a number of 5-membered and 6-membered heteroaryl groups. Notably, the pyridin-2-yl derivative was non-active. Thus some degree of consistency regarding the effect of the 5-nitrofuranyl group as the aryl unit in R-CONH–N=CH-aryl compounds is obtained.

3.2.3 Lipophilicities and toxicities

The lipophilicities of **1** and **2**, expressed as logP values, were determined using the Data Warrior program [70] (Table 3). Pharmacokinetic studies have indicated that a good balance between permeability and aqueous solubility for a drug is indicated by a logP value between 0 and 3. The value found for the most active compound of this study, **1f**, falls within this range, being 0.261. Other compounds that have outstanding activity are the heteroaromatic derivatives **2h** and **2i**: the log *P* values, 0.146 and 0.103, for these compounds also fall within the ideal range, but the values suggest that the compounds will be slightly more water soluble. The toxicities of the compounds **1** and **2** were also determined using the Data Warrior program [70] (Table 2). The most promising compound in each series, compounds **1f** and **2i**, were found to be non-mutagenic and non-tumorigenic.

3.3 Crystallography

3.3.1 General

Recrystallization of compounds, **1a** and **2d,** from moist methanol at room temperature produced anhydrous crystals, while that for **2e** generated the monohydrate – all from the same batch of methanol. Refinements of **1a** and **2e·(H$_2$O)** proceeded most satisfactorily, but not that of **2d**. As mentioned below and shown in Table 3, these are nearly planar π systems which allows for close packing with formation of stacks, or at least dimers, either with molecules in parallel or anti-parallel orientations. As the linker groups contain nitrogen donors (and oxygen donors for acylhydazones) and an C=N group, there is scope for π interactions between the layers in the stack, including of course π···π as well as C=O···π, N–H···π and C=N···π interactions, etc., depending on the offsets between successive molecules in successive layers of the stack.

Table 3: Selected bond lengths.[a]

Compound	C2–N3	N3–N4	N4–N7	C7–C11
(a) Hydrazones				
1a	1.3649(5)	1.3596(13)	1.2843(17]	1.4545(16)
Range of values found	1.3421(14)–	1.353(2)–	1.2700(15)–	1.439(7)–
for related compounds [64, 71–76]	1.381(3)	1.3730(12)	1.2919(15)	1.4800(14)

Compound	C2–C8	C8–O8	C8–N3	N3–N4	N4–C7	C7–C11
(b) Acylhydrazones						
2d	1.512(5)	1.212(4)	1.353(5)	1.373(4)	1.291(5)	1.451(5)
2e·(H$_2$O)	1.519(2)	1.2215(19)	1.349(2)	1.376(2)	1.287(2)	1.448(2)

[a]Standard bond lengths, Å: C–C 1.54, C=C 1.34, C–N 1.47, C=N 1.25, N–N 1.45, N=N 1.25, C–O 1.43, C=O 1.21 [71].

3.3.2 Compound 1a

The atom arrangement and numbering scheme and a side-on view of the conformation of compound **1a** are shown in Figure 2a: the intramolecular hydrogen bond, O12–H12···N4, is drawn as a dashed line. The molecule is slightly distorted from planarity as indicated by the interplanar angles. The interplanar angles indicate that the successive rotations of the linkers and rings occur in the same sense: the consequence of that is the overall slight curvature of the molecules as illustrated in Figure 2a. As shown in Table 3, a comparison of the measured bond lengths in the linker chain with standard bond lengths indicates delocalisation [71]. Also included in Table 3 are the equivalent bond lengths in related published structures [64, 72–76]: there are only small ranges for each bond length despite some variation in the compounds in terms of substituents, solvation and protonation.

The intermolecular interactions in compound **1a** are N–H···N and C–H···O hydrogen bonds and π···π and C–H···π interactions (Table 4). Pairs of the classical hydrogen bonds, N3–H3···N1, generate dimers with $R_2^2(8)$ rings [77]. Such dimers are linked into zig–zag chains by pairs of weaker C5–H5···O12 and C4–H4···H2 hydrogen bonds (Figure 3a and b). A side-on view of a chain indicates its slight undulating nature (Figure 3b). The connections by the C5–H5···O12 and C4–H4···H2 hydrogen bonds to the dimers with the N3–H3···N1 connectivity produce one $R_2^2(6)$ ring and two $R_2^2(12)$ rings. The chains, illustrated in Figure 3a, are linked into sheets by $\pi_A\cdots\pi_B$/ $\pi_B\cdots\pi_A$ and $\pi_A\cdots\pi_A$ interactions (Figure 3c). The former interactions are stronger as indicated by the smaller offsets and shorter Cg···Cg distances (Table 4). Molecules with $\pi_B\cdots\pi_A/\pi_A\cdots\pi_B$ interactions are lined up antiparallel. A similar situation pertains with the $\pi_A\cdots\pi_A$ interaction. The last sub-structure to mention is the chevron-type arrangement produced from the C13–H13···π interactions and C14–H14···O12 hydrogen bonds (Figure 3d). The C14–H14···O12 hydrogen bonds generate C(5) chains.

The hydroxyl group is thus involved in the intramolecular hydrogen bond with N4 and in two intermolecular C5–H5···O12 and C14–H14···O12 hydrogen bonds. All four nitrogen atoms are involved in several interactions, but in the case of N4, the only interaction is the intramolecular O12–H12···N4 interaction. Overall, compound **1A** has a two-dimensional structure.

3.3.3 Compound 2d

The resolution of the structure of compound **2d** was not perfect as indicated by the high R_1 and R_{int} values of 0.094 and 0.116, respectively: the ellipsoids were also fairly distorted. However, the CIF check indicated no A or B alerts. As attempts to gain better crystals failed and the fact that no related structure of an unhydrated pyrimidin-2-yl acyl hydrazone was in the CCDC data base, we still feel it is useful to elaborate on some of the structural details.

Figure 2b shows the atom arrangements and numbering scheme of the compound. The arrangement about the –C(O)NH–N=C- fragment is $(E)_{CONH}/(E)_{N=C}$ [69, 78]. The intramolecular hydrogen bonds, O12–H12···N4 and N3–H3···N2, are drawn as dashed lines. The molecule has a very slight S-shape, as indicated by the interplanar angles. Further details are summarized in Table 3.

The intermolecular interactions in compound **2d** as indicated by PLATON are O–H···O, C–H···N and C–H···O hydrogen bonds and C8=O8···π interactions (Table 4).

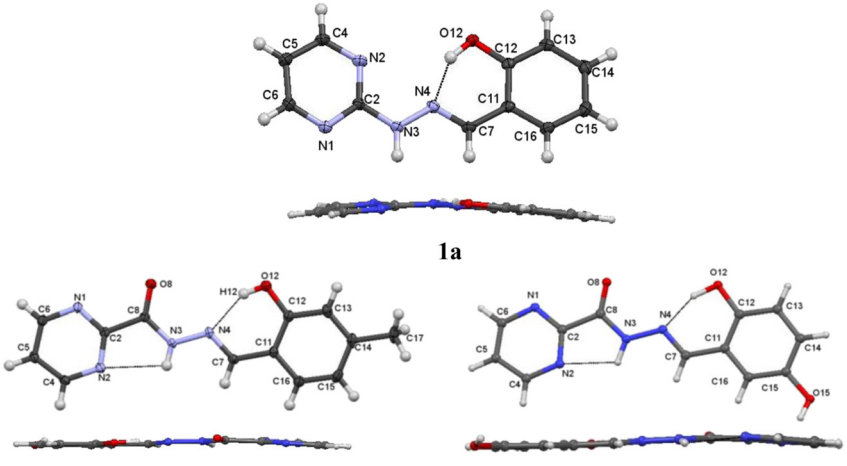

Figure 2: Atom numbering schemes and atom arrangements.

Table 4: Geometric parameters (Å, deg) for intra- and intermolecular interactions.

Compound	D–H···A	D–H	H···A	D···A	D–H···A	
(a) Intramolecular hydrogen bonds						
1a	O12–H12···N4	0.899(18)	1.790(18)	2.6004(13)	148.8(14)	
2d	N3–H3···N2	0.92(4)	2.11(4)	2.596(5)	111(3)	
2d	O12–H12···N4	0.96(5)	1.70(5)	2.611(4)	157(3)	
2e·(H_2O)	N3–H3···N2	0.84(2)	2.364(19)	2.705(2)	105.1(15)	
2e·(H_2O)	O12–H12···N4	0.84(2)	1.87(2)	2.6368(19)	151(2)	
Compound	**D–H···A**	**D–H**	**H···A**	**D···A**	**D–H···A**	**Symmetry code**
(b) Intermolecular hydrogen bonds						
1a	N3–H3···N1	0.908(14)	2.080(14)	2.9848(15)	174.1(13)	$1-x, 2-y, -z$
1a	C4–H4···N2	0.95	2.60	3.4218(17)	144	$1-x, 1-y, -z$
1a	C5–H15···O12	0.95	2.61	3.2252(16)	125	$1-x, 1-y, -z$
1a	C14–H14···O12	0.95	2.64	3.3832(16)	119	$½-x, -½+y, ½-z$
2d	O15–H15···O8	0.85(5)	1.95(5)	2.761(4)	159(4)	$-1+x, ½-y, -½+z$
2d	C16–H16···O8	0.95	2.44	3.125(5)	129	$-1+x, ½-y, -½+z$
2d	C7–H7···O12	0.95	2.43	3.333(5)	158	$-1+x, ½-y, -½+z$
2d	C13–H5···O15	0.95	2.61	3.509(5)	158	$1+x, -y, ½+z$
2d	C5–H13···N2	0.95	2.55	3.206(5)	126	$1-x, -½+y, ½-z$
2e·(H_2O)	OW–H1···N1	0.84(2)	2.08(2)	2.9106(19)	172(2)	$½-x, -½+y, ½-z$
2e·(H_2O)	OW–H2···N2	0.84(2)	2.17(2)	2.9322(19)	151(2)	x, y, z
2e·(H_2O)	N3–H3···OW	0.84(2)	2.11(2)	2.9406(19)	172.5(17)	x, y, z
2e·(H_2O)	C4–H4···O8	0.93	2.51	3.1778(18)	129	$-½-x, -½+y, ½-z$
Compound	**Y–X···Cg[a]**	**X···Cg**	**X_{perp}**	**γ**	**Y–X···Cg**	**Y···Cg**	**Symmetry code**
(c) Y–X···π interactions[a]							
1a	C13–H13···Cg2	2.9–(18)	2.87	7.91	137	3.6438(14)	$x, ½-y, ½+z$
2d	C8–O8··· Cg1	3.523(4)	3.362	17.37	74.2(2)	3.398(14)	x, y, z
2e·(H_2O)	C17–H17A··· Cg2	2.75	2.62	17.57	148	3.599(2)	$1+x, y, z$
2e·(H_2O)	C8–O8··· Cg1	3.8911(13)	3.544	24.38	61.16(8)	3.4709(16)	$1+x$, y, z
Cg(I)···Cg(J)	**Cg···Cg**	**α**	**β**	**γ**	**CgI_{perp}**	**CgJ_{perp}**	**Symmetry code**
(d) π···π interactions							
1a	Cg(1)···Cg(2)	3.8841(9)	12.18(6)	29.5	24.7	3.5298(5)	3.3794(5)	$-x, 1-y, -z$
1a	Cg(1)···Cg(1)	4.1580(10)	0.00(6)	29.0	29.0	3.6381(5)	3.6382(5)	$1-x, 2-y, -z$

Cg(I) and Cg(2) = centres of gravities of pyridinyl and phenyl rings of the quinoline ring, respectively; α = dihedral angle between planes *I* and *J* (deg); β = angle Cg(*I*) → Cg(*J*) (deg); γ = angle between Cg(*I*) → Cg(*J*) vector and normal to plane *J* (deg); Cg–Cg = distance between ring Centroids (Å); Cg–I_{perp} = perpendicular distance of Cg(*I*) on ring *J* (Å).

Molecules of the acylhydrazone are linked into columns by combinations of O15–H15···$O8_{(carbonyl)}$, C16–H16···$O8_{(carbonyl)}$, C7–H7···$O12_{(hydroxy)}$ and C13–H13···N2 hydrogen bonds: alternating molecules in the columns are positioned anti-parallel. Such columns are further linked into sheets by C5–H5···$O15_{(hydroxy)}$ hydrogen bonds (Figure 4a): alternating molecules in layers of the sheet are inverted. The sheets are composed of a series of rings with the symbols $R_2^2(11)$, $R_2^2(13)$, $R_3^2(6)$, and $R_4^4(18)$. Another view, looking down the *b* axis, a portion of the twisted, undulating sheet is shown in Figure 4b. The sheets are linked into a three-dimensional array by carbonyl···π (C8=O8···π) interactions, an example of the interaction is shown in Figure 4c. The carbonyl oxygen atom is thus involved in three intermolecular interactions, the π interaction, as above, and the two C–H···O hydrogen bonds forming the $R_3^2(6)$ ring. The C8=O8···π interactions occur between acylhydrazone molecules in different layers as shown in Figure 4c: in such an arrangement, the N3–H3 moiety is situated above a phenyl ring, resulting in a T shaped arrangement for the N3–H3···π_B interaction (with d(H–Cg_B) = 3.44 Å and ∠N–H···Cg_B = 77° (Figure 4d) [79–81].

The hydroxyl group on C12 is involved in a intramolecular O12–H12···N4 hydrogen bond and in two intermolecular C–H···O hydrogen bonds, while the hydroxyl group on C15 plays a lesser role being solely involved in linking the chains into sheets. In contrast to the hydrazonyl compound **1a** the nitrogen atom N2 in the pyridinyl ring is

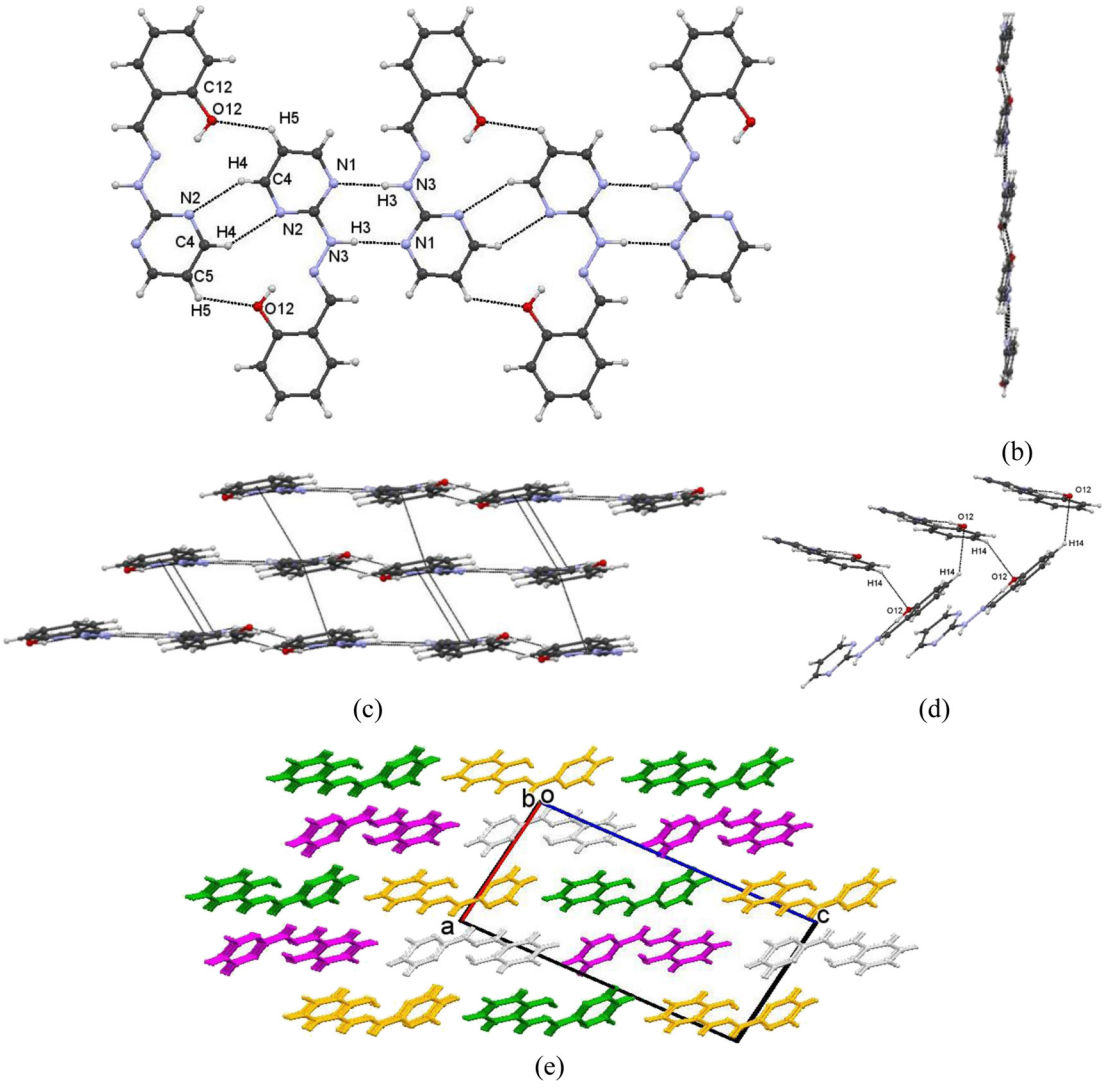

Figure 3: Compound **1a**.
(a) Part of a chain of molecules formed from C5–H5···O12, C4–H4···N2, C5–H5···O12 and C4–H4···N2 hydrogen bonds, (b) a side-on view showing the slight undulating nature of the chain, (c) part of a 2-dimensional array of molecules formed from linking the chains, shown in Fig.5a, by $\pi_A\cdots\pi_B$ and also $\pi_A\cdots\pi_A$ interactions, (d) a chevron-type arrangement produced from the C13–H13···π interactions and C14–H14···O12 hydrogen bonds, (e) packing of molecules looking down the *b* axis: differently coloured molecules indicate different operations.

not involved in intermolecular interactions, but is utilized in the intramolecular hydrogen bond with the ortho hydroxyl group on C12. Compared to the situation in compound **1a**, the presence of the carbonyl group in the acylhydrazone derivative results in the suppression of any intermolecular activity of this nitrogen atom.

A view of the packing of the molecules is illustrated in Figure 4e, looking down the *b* axis.

3.3.4 Compound 2e·(H_2O)

The atom arrangement and numbering scheme and a side-on view of the conformation of **2e·(H_2O)**, are shown in Figure 2c: the intramolecular hydrogen bonds, O12–H12···N4 and N3–H3···N2, are drawn as dashed lines. The arrangement about the –C(O)NH–N=C- fragment is $(E)_{CONH}/(E)_{N=C}$ [69, 78]. The molecule is non-planar as shown by the interplanar angles as in **2d**, the acylhydrazone molecule in **2e·(H_2O)**, also has a slight S-shape. Further details are summarized in Table 3 [71].

The intermolecular interactions in compound **2e** are OW–HW···N, N–H···OW and C–H···O hydrogen bonds and C8=O8···π_A and C17–H17A···π_B interactions (Table 4). The water molecules indirectly link the acylhydrazone molecules into chains, via N3–H3···Ow, Ow–H2···N2 and Ow–H2···N2 hydrogen bonds (Figure 5a). A view of a chain

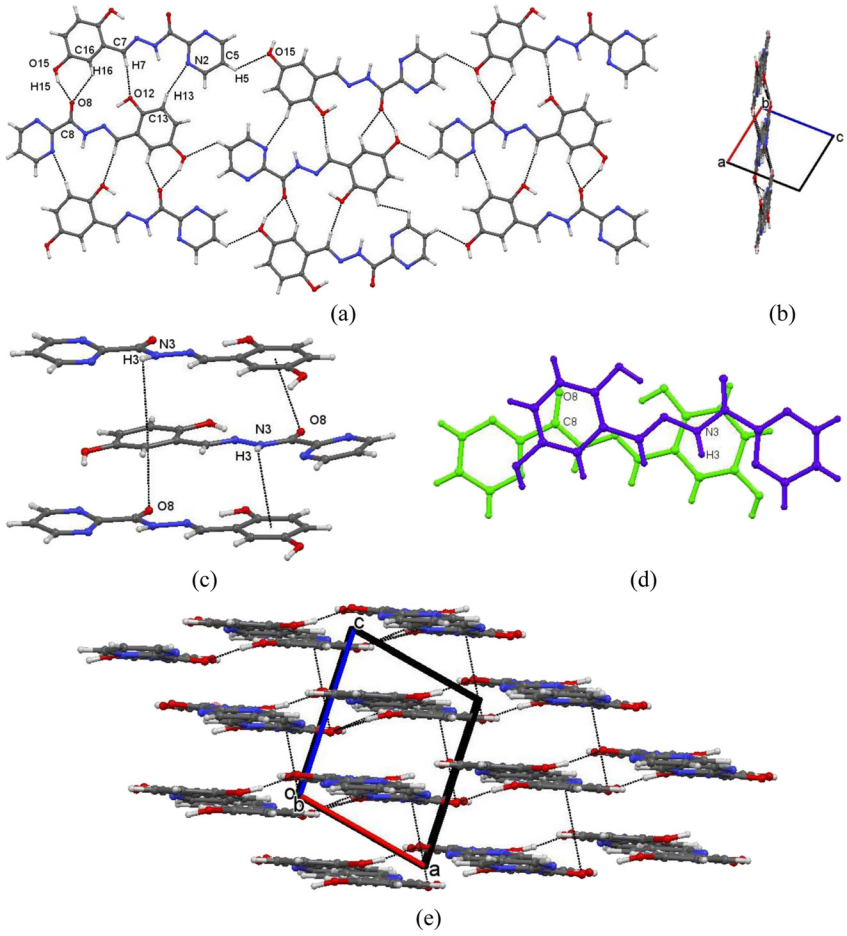

Figure 4: Compound **2d**.
(a) Part of a sheet of molecules formed from O15–H15···O8(carbonyl), C16–H16···O8(carbonyl), C7–H7···O12(hydroxy), C13–H13···N2 and C5–H5···O15 hydrogen bonds (b) another view, looking down the *b* axis, of the portion of the twisted, undulating sheet shown in Figure 4a, (c) carbonyl·π (C8=O8···π) interactions, which combine with the sheets, to form a three-dimensional array, (d) a view of the overlap of acylhydrazone molecules in successive rows of the stack shown in Figure 4c, showing the positioning of the N–H moiety over a phenyl ring, (e) a view of the packing of the molecules, looking down the *b* axis.

indicating its undulating nature is shown in Figure 5b. Within the chain, $R_2^3(7)$ rings are formed from the combination of the Ow–H2···N2 and N3–H3···Ow hydrogen bonds. Successive acylhydrazone molecules in the chain are anti-parallel.

PLATON revealed C8=O8···π_A and C17–H17A···π_B interactions linking stacks of molecules, in which successive molecules are off-set by 3.25 Å, but orientated in the same sense (Figure 5c). The offset is required to accommodate the C17–H17A···π_B interactions – and places the C=N moiety in an ideal position to form a C=N···π interaction with a phenyl ring in the next layer, $Cg_{(C=N)}\cdots Cg_{(PhB)}$ = 3.41 Å (Figure 5c). Figure 5d illustrates the extensive overlap of three molecules in consecutive layers of a π stack. These π stacks are linked into two-dimensional arrays by C4–H4···$O8_{(carbonyl)}$ hydrogen bonds (Figure 5e): the molecules drawn in different colours are related by different symmetry operations. Figures 5e and f provide two views of the interactions, both the indirect acylhydrazone-acylhydrazone links, involving the water molecules, and the direct acylhydrazone-acyl hydrazone links. Water molecules are drawn in red and the acylhydrazone molecules either in green or blue, depending on their symmetry relation. Each acylhydrazone molecule is linked to molecules in the same row and to molecules in both the rows above and below in a spiral arrangement. Each water molecule is connected to two acylhydrazone molecules (Figure 6).

3.3.5 Comparisons of structures of 2d and 2e·(H_2O)

The conformations of the acylhydrazone molecules in **2d** and **2e·(H_2O)** are very similar (Figure 3). However, the presence of the water molecules in **2e·(H_2O)** results in marked differences in the structures. These water molecules are only involved in the formation of hydrogen bonded chains indirectly linking acylhydrazone molecules, while connections between these chains and the direct links between acylhydrazone molecules are provided by C–H···$O_{(carbonyl)}$ and by both C–H···π and C=O···π interactions: the latter is also present in anhydrous **2d**, but the C–H···π interaction is absent. The C=O···π interactions provide the direct links between the hydrogen bonded sheets of the acylhydrazone molecules in **2d**, which result

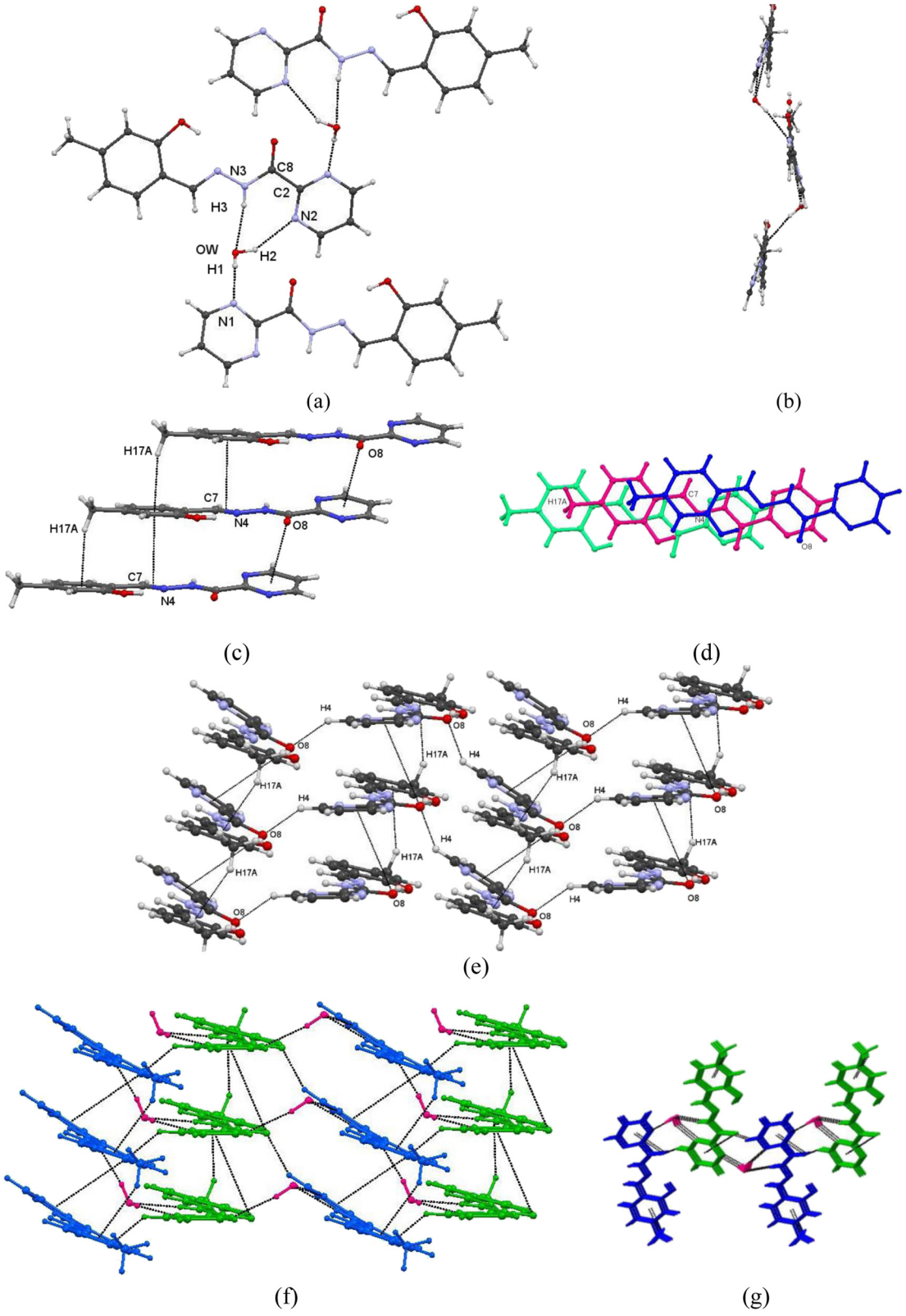

Figure 5: Compound **2e·(H_2O)**.
(a) Part of a column of acylhydrazone molecules linked indirectly by water molecules, utilizing N1–H1···Ow, Ow–H2···N2 and N3–H3···OW hydrogen bonds, (b) a side-on view of the column shown in Figure 5a, (c) part of a stack of acylhydrazone molecules formed from C8=O8···π_A, C17–H17A···π_B and $\pi_{(C=N)}$ ··$\pi_{(PhB)}$ interactions, (d) overlap of three consecutive layers of molecules in the π stack, (e) arrangement of the acylhydrazone molecules formed from linking the π stack by C4–H4···O8 hydrogen bonds, (f) and (g) two views of the arrangement of linked acylhydrazone and water molecules: water molecules are drawn in red and acylhydrazone molecules in green or blue, depending on the symmetry operation.

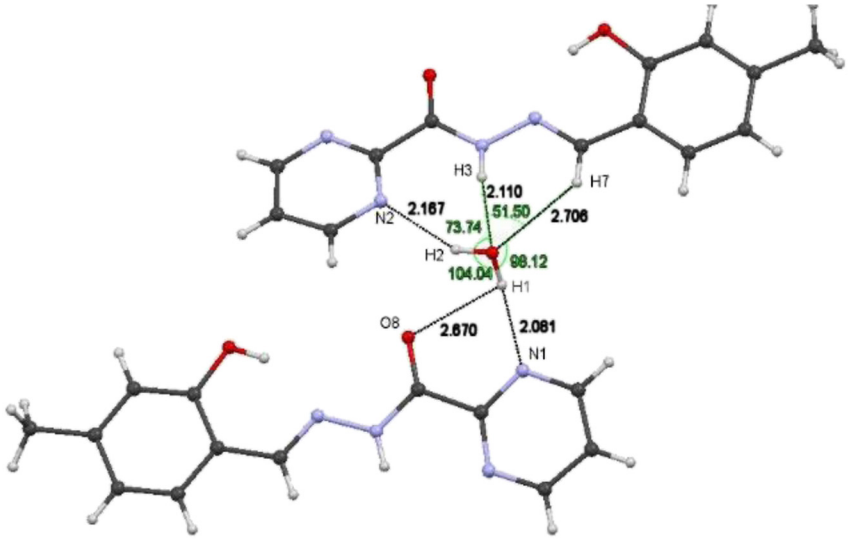

Figure 6: Compound **2e·(H_2O)**. The arrangement around the water molecule: angles and distances calculated using the MERCURY program.

in a three-dimensional structure. The different arrangements of the layers in the stacks in **2d** and **2e·(H_2O)**, result in different sets of π interactions.

3.3.6 Comparisons with reported structures

The search of the CCDC data base on 29th April 2020 [49] indicated very few structures of pyrimidin-2-ylhydrazones: the only known structures of pyrimidin-2-ylacylhydrazones are the two reported in this article. For the substructure, 2-(C–C=N–NH)-1,3-$N_2C_4H_3$, only 13 different hits are found, in addition to our compound **1a** (Table 5). In Table 5, the numbering scheme used follows that employed for **1a** and could thus be different from that used in the original reports. In the discussion which follows, the emphasis is on the main intermolecular interactions involving the hydrazone moiety, the hydroxyl groups, if any, and the π interactions.

3.3.7 Hydrazones

All the pyrimidin-2-ylhydrazone structures reported herein have an (*E*) configuration about the N4–C7 bond, as generally most hydrazones do in the solid state, a consequence of the much greater stability of the (*E*) form over the (*Z*) form. Due to the fact that rotations around the C2–N3 and C7–C11 bonds require less energy, compounds with unsymmetrically substituted pyrimidin-2-yl and phenyl groups can adopt different conformations, as revealed below.

For each of the compounds, bar one, in Table 5, the core of the hydrazone molecule, consisting of the non-hydrogen atoms making up the aryl rings and the linker chain, has a slightly distorted planar conformation, no matter whether the hydrazone is protonated or solvated or just a neutral compound: interplanar angles between the terminal aryl groups are less than 12°, the one exception being one of the two independent molecules of compound **3** [19.98(10)°], a sterically hindered compound with additional aryl groups, including fused groups (entry 5 in Table 5).

Just two of the compounds in Table 5 are anhydrous derivatives with a 2-hydroxyphenyl group, and are thus most similar to compound **1a**. These compounds are 2-methoxy-6-({2-[4-(trifluoromethyl)pyrimidin-2-yl]hydrazinylidene}methyl)phenol, **4** [CCDC codes: SIFNON: 1544930] [73] and 2-(*N*-(4,6-dimethyl-2-pyrimidinyl)ethanehydrazonoyl)phenol, **5** [CCDC codes: BOSCIW, 678939] [74]. In these compounds, as in compound **1a**, intramolecular O–H···N1 hydrogen bonding involving the 2-hydroxy group fixes the conformation about the C2–N3 bond.

In crystals of compounds **1a** and **5**, there are strong intermolecular N3–H3···N1 interactions, pairs of which create $R_2^2(8)$ dimers (central part of Figure 2a). These dimers are further linked into three-dimensional structures by π···π interactions and by weaker interactions, such as C–H···O and C–H···π. For compound **1a**, the symmetric dimers are very nearly planar as there are no substituents present to cause any steric hindrance. However, in **5** with its two independent molecules, the asymmetric dimers have an interplanar angle of 60.5° between the two monomeric units. With the conformation at the C2–N3 bond fixed in both monomeric units to allow the intramolecular O–H···N1 hydrogen bond, methyl groups at both the pyridinyl and phenyl rings are placed on the sides in each molecule to minimise the steric consequences.

A very significant difference is found in **4**: here tetramers are generated from the two independent molecules through

Table 5: Selected details of published pyrimidin-2-yl hydrazones.

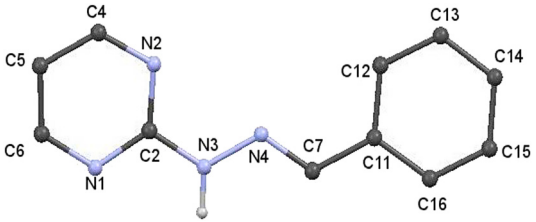

Entry no.	Compound	Conformation	Main interactions and structural details	Interplanar angles (deg)[a]	CCDC Codes [Reference]
1	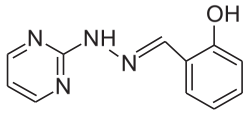 Compound **1a**	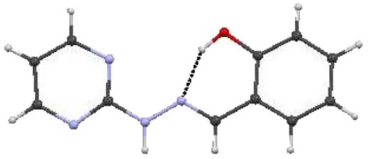	Intramolecular O12–H12···N4 hydrogen bond, Pairs of N3–H3···N1 hydrogen bonds generate near planar dimers, with $R_2^2(8)$ rings, linked into chains by pairs of C5–H5···O12 and C4–H4···N2 hydrogen bonds, further linked by π···π interactions	12.18(6)	HISXOZ This study
2	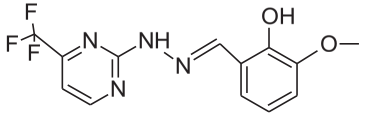 Compound **4**	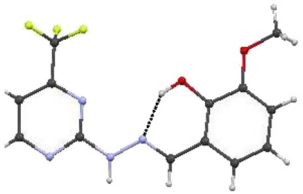	Two independent molecules: Intramolecular O12–H12···N4 hydrogen bond Tetrameric units formed from N3–H3···N1 and π···π, units linked into 3-D array by C–F···π, C–H···F and C–H···N interactions.	12.45(11) 7.31(14)	SIFNON 1544930 [73]
3	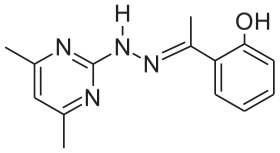 Compound **5**	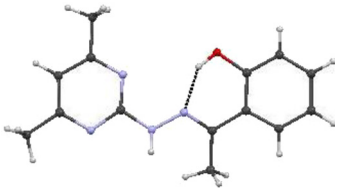	Two independent molecules: Intramolecular O1–H1···N4 hydrogen bond. Pairs of N3–H3···N1 hydrogen bonds generate non-planar dimers, with $R_2^2(8)$ rings; links by π···π, C–H···π interactions and C–H···O hydrogen bonds provide a 3-D array	1.32(7) 3.34(6)	BOSCIW 678939 [74]

Table 5: (continued)

Entry no.	Compound	Conformation	Main interactions and structural details	Interplanar angles (deg)[a]	CCDC Codes [Reference]
4	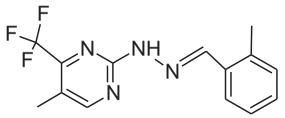 Compound **6**	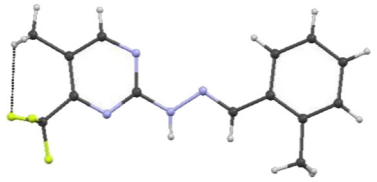	N3–H3···N1 hydrogen bonds, augmented by C–H···N1 hydrogen bonds, form chains: molecules in chains are rotated alternatively by 83.9 and 37.9°, respectively; π···π interactions and C–F···π are present.	10.5(8)	TOLJEK 683535 [75]
5	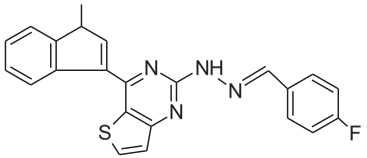 Compound **3**	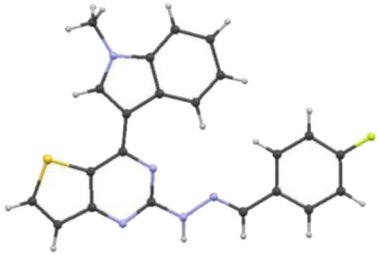	Two independent molecules. Pairs of N3–H3···N1 hydrogen bonds generate non-planar asymmetric dimers, with $R_2^2(8)$ rings[angle between monomers = 54.5°] dimers are linked by π···π, C–H···π interactions, S···F contacts, C–H···N hydrogen bonds etc.	12.47(10) 19.89(10)	FOQPEJ 1908708 [72]
6	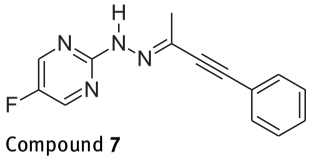 Compound **7**	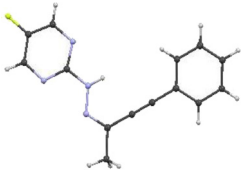	No π···π interactions. Two molecule-wide planar networks formed from C–H···Nl, C–H···N4 and C–H···F hydrogen bonds, are linked by C–F···π and C–H···π interactions.	7.66(16)	POVJES 1903453 [76]
7	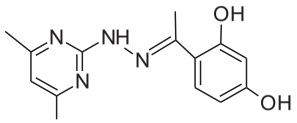 HYDRATE Compound **8**	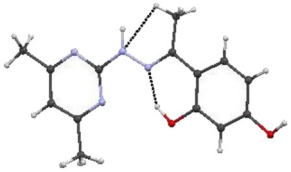	Intramolecular O12–H12···N4 and C–H···N3 hydrogen bonds; each water molecule is linked to 3 hydrazones, thereby creating undulating sheets: π···π, C–H···π, C–H···O link sheets into a 3-D arrangement: possible N–H···π interaction:]H···Cg_{Ph} = 3.62 Å, ∠N–H···Cg_{Ph} = 81°.	4.47(5)	DUWJEM 1015148 [64]

Table 5: (continued)

Entry no.	Compound	Conformation	Main interactions and structural details	Interplanar angles (deg)[a]	CCDC Codes [Reference]
8	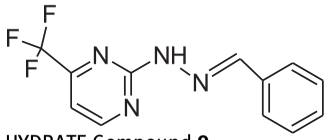 HYDRATE Compound **9**	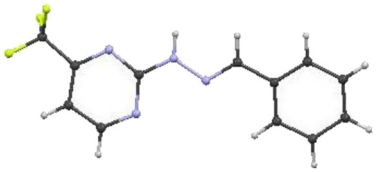	Water indirectly links hydrazine molecules into chains using Ow–Hw···N1, N3–H3···Ow and weaker C–H···Ow hydrogen bonds: chains are linked by π···π, C–H···F and C–H···O interactions: possible $\pi_{(C=N)}\cdots\pi_{Ph}$ interaction $N\cdots Cg_{Ph}$ = 3.48Å	8.43(7)	TOLJIO 683536 [75]
9	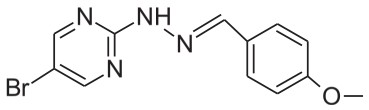 HYDRATE Compound **10**	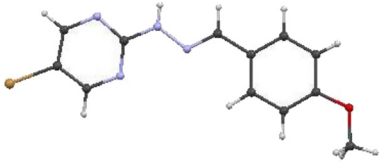	Water connects to three hydrazone molecules. These tetrameric clusters are further linked by water and strong π···π interactions.	10.68(8)	SABLUE 792526 [82]
10	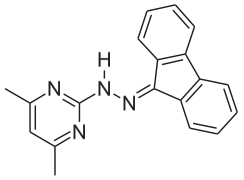 DIHYDRATE Compound **11**	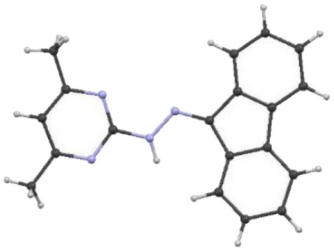	Hydrogen atoms in the water molecules are not refined: π···π linked dimers are indirectly connected into columns by a set of four water molecules via hydrogen bonds involving water and N3–H3/N1/ C–H centres. The four water molecules form a planar cyclic tetramer. Such columns are liked into 2-molecule wide sheets by further π···π interactions: weak interactions between the sheets: C–H···π.	3.80(12)	KEZCOK 105046 [83]

Table 5: (continued)

Entry no.	Compound	Conformation	Main interactions and structural details	Interplanar angles (deg)[a]	CCDC Codes [Reference]
11	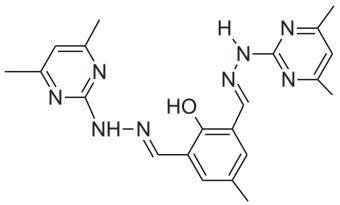 EtOH solvate Compound **12**	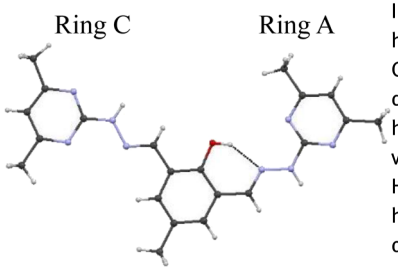	Intramolecular O12–H12···N4 hydrogen bond. Chains of molecules are formed directly from N3A–H3A···N1 hydrogen bonds and indirectly via the solvate molecule [O1S–H1S···N1 and N3B–H3B···O1S hydrogen bonds]: The zig-zag chains containing $R_3^3(10)$ rings and have ca. 120° angles between successive molecules in the chain. C–H(solvate) ···π interactions	11.41(17) 5.77(17)	LIYNIT 1845762 [84]
12	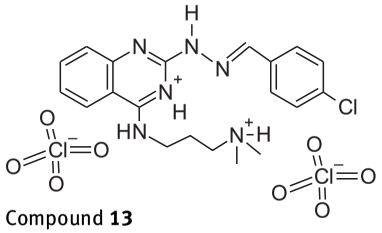 Compound **13**	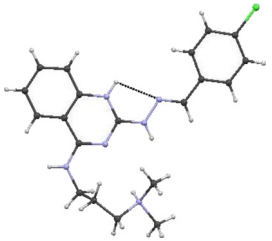	Intramolecular N1–$H1^+$···N4 hydrogen bond [$(dication)_2(-ClO_4)_2]^{2+}$ units are formed from π···π interactions and three N–H···O(ClO_3) hydrogen bonds, using the two protonated nitrogen centres and the N3–H3 moiety: these units are linked by ClO_4^- anions via C–H···O hydrogen bonds, and by C–H···π and Cl–O···π interactions<	2.97(16)	ZARGUW 866280 [85]
13	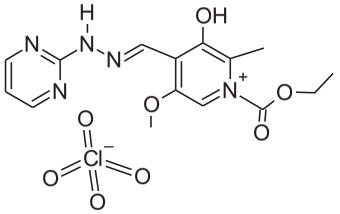 Compound **14**	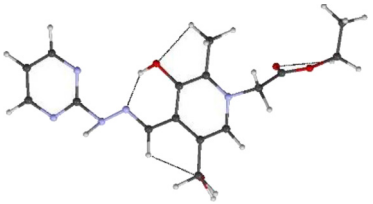	Intramolecular O–H···N1 hydrogen bond: no π···π interactions: dimers of the cation are formed by pairs of (CH_2)O–H···N1 hydrogen bonds to give $R_3^3(20)$ rings; interactions, C–H···π	1.50(5)	LENQEA 1205521 [86]

strong N3–H3···N1 and N3–H3···O1 hydrogen bonds and strong π···π interactions [$Cg_A \cdots Cg_B$ = 3.6326(16) Å and slippages of 1.124 and 1.260 Å]. The formation of the tetramers can be considered to arise from linking the different molecules via a N3A–H3A···N1B hydrogen bond to yield an asymmetric dimer, with an inter-planar angle of near 87°, which is further linked to another dimer, involving N3B–H3B···O1A hydrogen bonds and $\pi_A \cdots \pi_B$ interactions. Further π···π interactions and C–H···F and C–H···N interactions link the tetramers into a three-dimensional array. As can be seen in Table 4, entry number 2, the conformation adopted does not explain why there is no N3–H3···N1 linked dimer, as the sides of the molecules which would be linked in such a dimer are free of any bulky group.

The principal hydrogen bond in ((methylbenzylidene) hydrazinyl)-5-methyl-4-(trifluoromethyl)pyrimidine, **6** [Table 5, entry no. 4], a compound without a 2-hydroxy group, is also the N3–H3···N1 hydrogen bond. However in this case, chains are formed rather than $R_2^2(8)$ dimers. The conformation of **6**, about the C7–C12 bond, and the positioning of the trifluoromethyl group indicate that dimer formation, involving pairs of N3–H3 units, would create significant steric hindrance. Although compound **3** [Table 5, entry no. 5] has no fused aromatic rings, it does have a conformation which allows the formation of N3–H3···N1 linked non-planar dimers with a relatively large angle of 54.5° between the best planes through the different monomer units.

Compound **7** [Table 5, entry no. 6], with a different type of hydrazone unit, has a different set of intermolecular interactions. No N–H···N hydrogen bonds or π···π interactions are detected, but various C–H···N, C–H···π and C–H···F hydrogen bondsforming essentially separated planar sheets.

The remaining compounds in Table 5 are either solvates or protonated pyrimidinyl compounds. In the case of the solvates, the solvate molecule is very strongly involved in the intermolecular interactions with consequential indirect hydrazone–hydrazone contacts. The involvement of the water molecule varies strongly with the substituents in the hydrazine. In most cases, π···π interactions remain important. As expected, water has a more significant impact then does ethanol, and the effect of two molecules of water is more dramatic than that of just one (compare entry 10 with entries 7–9). The perchlorate salts, entries 12 and 13, exhibit various intermolecular interactions, including N–H···O(ClO_3) hydrogen bonds. The salt **8** maintains π···π interactions, whereas the salt **9** maintains the intramolecular O12–H12···N1 hydrogen bond, indicating the importance of such interactions, where appropriate, also in the pyrimidin-2-yl hydrazones.

4 Conclusions

While the anti-mycobacterial activities of the compounds studied cover a large range, there is sufficient indication that further study would be useful. The most active compounds were (*E*)-5-nitro-2-((2-(pyrimidin-2-yl)hydrazono) methyl)phenol, **1f**, and **(***E***)-*N*′-((5-nitrothiophen-2-yl)methylene)pyrimidine-2-carbohydrazide, **2i**, with different substituents in the aryl moiety. A comparison of the effect of the substituents at the aryl group on the anti-TB activities in other heteroarylhydrazone compounds, Ar-CH=N–NH-heteroaryl indicated a range of activities, i.e., there was no consistent influence of the Ar groups on the activities. With the pyrimidinyl compounds, **1**, the results indicated that the donor abilities of the Ar group, [e.g. 2-hydroxyphenyl or pyridine-2-yl], was not of prime importance. In contrast with Ar-CH=N–NH–CO-heteroaryl compounds, cases with Ar = 5-nitrofuran-2-yl generally produce the more active compounds.

While there have been few reports of the structures of pyrimidin-2-yl hydrazones, some general conclusions can still be made. There is a very strong indication of the importance of the N3–H3 hydrogen bonding, either to form dimers, especially in the absence of steric effects, or chains. There is also a strong indication that π interactions, especially π···π interactions, are an important feature, especially in linking sheets and chains of molecules, formed primarily from hydrogen bonding interactions. Even *N*-protonated and solvated compounds show a propensity to maintain intramolecular O12–H12···N1 hydrogen bonds in hydrazones formed from 2-hydroxybenzaldehyde precursors and to possess π···π interactions. The influence of solvate molecules on the structures is very significant through the formation of many indirect links between the hydrazones.

There are even fewer reports of the structures of pyrimidin-2-ylacyl hydrazones. Here too, O12–H12···N1 hydrogen bonds in acylhydrazones formed from 2-hydroxybenzaldehyde precursors prevail, but not $\pi_{(aryl)} \cdots \pi_{(aryl)}$ interactions. However, due to the fact that the molecules, contain potential donor sites, e.g., nitrogen and oxygen groups, and a C=N moiety, can form stacks with parallel or antiparallel arrangements, with different offsets, other π interactions can arise, such as N–H···π, C=O···π, C–O···π and or C=N···π, as found in **2d** and **2e·(H$_2$O)**. The hydrazine compound **1a** exhibited $\pi_{(aryl)} \cdots \pi_{(aryl)}$, but apart from C–H···π interactions, did not exhibit any X–Y···π interactions. However, the hydrazonyl compounds, **8** and **9**, entries 7 and 8, in Table 5, do: compound **8** exhibits a N–H···$Cg_{(Ph)}$ interaction and compound **9** a $\pi_{(C=N)} \cdots \pi_{(Ph)}$ interaction. Thus it is also a

feature found in pyrimidin-2-ylacyl hydrazones, with a suitable positioning of the molecules in the stacks.

5 Supporting information

CCDC 2008878, 2008885 and 2008879 for **1a**, **2d** and **2e·(H_2O)**, respectively, contain the supplementary crystallographic data for this paper. These data can be obtained free of charge from The Cambridge Crystallographic Data Centre via http://www.ccdc.cam.ac.uk/data_request/cif. The details of the crystal structure determinations in cif format are also available in the online version (https://doi.org/10.1515/znb-2020-0108).

Acknowledgements: The authors thank the National Crystallographic Service, University of Southampton for the data collection, and for their help and advice.
Author contribution: All the authors have accepted responsibility for the entire content of this submitted manuscript and approved submission.
Research funding: None declared.
Conflict of interest statement: The authors declare no conflicts of interest regarding this article.

References

1. Sahu M., Siddiqui N. *Int. J. Pharm. Pharm. Sci.* 2016, *8*, 8.
2. Panneer S. P., Richa J. C., Vijaysarathy D. P., Karyn V. S. *Res. Pharm.* 2012, *2*, 1.
3. Prachayasittikul S., Pingaew R., Worachartcheewan A., Sinthupoom N., Prachayasittikul V., Ruchirawat S., Prachayasittikul V. *Mini-Rev. Med. Chem.* 2017, *17*, 869.
4. Liu X., Feng T., Wang D., Liu H., Yang C., Li X., Lin B., Zhao Z., Zhou Y. *Tetrahedron Lett.* 2016, *57*, 4113.
5. Tian C., Wang M., Han Z., Fang F., Zhang Z., Wang X., Liu J. *Eur. J. Med. Chem.* 2017, *138*, 630.
6. Gregorić T., Sedić M., Grbčić P., Paravić A. T., Paveli S. K., Cetina M., Vianello R., Raić-Malić S. *Eur. J. Med. Chem.* 2017, *125*, 247.
7. Negi B., Rawat D. S. *Med. Res. Rev.* 2013, *33*, 693.
8. Zuniga E. S., Korkegian A., Mullen S., Hembre E. J., Ornstein P. L., Cortez G., Biswas K., Kumar N., Cramer J., Masquelin T., Hipskind P. A., Odingo J., Parish T. *Bioorg. Med. Chem.* 2017, *25*, 3922.
9. Singh K., Kaur T. *MedChemComm* 2016, *7*, 749.
10. Akula H. K., Kokatla H., Andrei G., Snoeck R., Schols D., Balzarini J., Yang L., Lakshman M. K. *Org. Biomol. Chem.* 2017, *15*, 1130.
11. Anthony N. G., Baiget J., Berretta G., Boyd M., Breen D., Edwards J., Gamble C., Gray A. I., Harvey A. L., Hatziieremia S., Ho K. H., Huggan J. K., Lang S., Llona-Minguez S., Luo J. L., McIntosh K., Paul A., Plevin R. J., Robertson M. N., Scott R., Suckling C. J., Sutcliffe O. B, Young L. C., Mackay S. P. *J. Med. Chem.* 2017, *60*, 7043.
12. Sankarganesh M., Raja J. D., Sakthikumar K., Solomon R. V., Vijayakumar V. *Bioorg. Chem.* 2018, *81*, 144.
13. Atta K. F. M., Ibrahim T. M., Farahat O. O. M., Al-Shargabi T. Q., Marei M. G., Bekhit A. A., El Ashry E. S. H. *Future Med. Chem.* 2017, *9*, 1913.
14. Chaturvedi R. N., Arish M., Kashif M., Kumar V., Reenu P. K., Rub A., Malhotra S. *Chem. Select.* 2018, *3*, 2756.
15. Wahbeh J., Milkowski S. *SLAS Technol.* 2019, *24*, 161.
16. Guimaraes D. G., Rolim L. A., Gonsalves A. D., Araujo C. R. M. *Rev. Virtual Quim* 2017, *9*, 2551.
17. Verma G., Marella A., Shaquiquzzaman M., Akhtar M., Ali M. R., Alam M. M. *J. Pharm. BioAllied Sci.* 2014, *6*, 69.
18. Singh N., Ranjana R., Kumari M., Kumar B. *Int. J. Pharm. Clin. Res.* 2016, *8*, 162.
19. Rodrigues F. A. R., Oliveira A. C. A., Cavalcanti B. C., Pessoa C. O., Pinheiro A. C., de Souza M V. N. *Sci. Pharm. J.* 2014, *82*, 21.
20. Bispo M. L. F., Alcântara C. C., Moraes M. O., Pessoa C. O., Rodrigues F. A. R., Kaiser C. R., Wardell S. M. S. V., Wardell J. L., de Souza M. V. N. *Monatsh. Chem.* 2015, *146*, 2041.
21. Rodrigues F. A. R., Bomfim I. S., Cavalcanti B. C., Pessoa C. O., Wardell J. L., Wardell S. M. S. V., Pinheiro A. C., Kaiser C. R., Nogueira T. C. M., Low J. N., Gomes L. R., de Souza M. V. N. *Bioorg. Med. Chem. Lett* 2014, *24*, 934.
22. Guerreiro D. D., Lima L. F., Sá N. A. R., Mbemya G. T., Ferreira A. C. A., Alves B. G., Maranhao S. S., Pessoa C. Ó., Pinheiro A. C., Nogueira T. C. M., de Souza M. V. N., de Figueiredo J. R., Rodrigues A. P. R. *Res. Vet. Sci.* 2020, *128*, 261.
23. Maranhão S. S., Moura A. F., Oliveira A. C. A., Lima D. J. B., Barros-Nepomuceno F. W. A., Paier C. R. K., Pinheiro A. C., Nogueira T. C. M., de Souza M. V. N., Pessoa C. *Bioorg. Med. Chem. Lett* 2020, *30*, 126851.
24. Alves M. S. D., das Neves R. N., Sena-Lopes A., Domingues M., Casaril A. M., Segatto N. V., Nogueira T. C. M., de Souza M. V. N., Savegnago L., Seixas F. K., Collares T., Borsuk S. *Parasites Vectors* 2020, *13*, 59.
25. Coimbra E. S., de Souza M. V. N., Terror M. S., Pinheiro A. C., Granato J. T. *Eur. J. Med. Chem.* 2019, *184*, 111742.
26. Coimbra E. S., Antinarelli L. M. R., Crispi M.de A., Nogueira T. C. M., Pinheiro A. C., de Souza M.V.N. *ChemMedChem* 2018, *13*, 1387.
27. Zanatta N., Amaral S.S., dos Santos J. M., de Mello D. L., Fernandes L. S., Bonacorso H. G., Martins M. A. P., Andricopulo A. D., Borchhardt D. M. *Bioorg. Med. Chem.* 2008, *16*, 10236.
28. Candea A. L. P., Ferreira M. L., Pais K. C., Cardoso L. N. F., Kaiser C. R., Henriques M. G. M. O., Lourenço M. C., Bezerra F. A. F. M., de Souza M. V. N. *Bioorg. Med. Chem. Lett.* 2009, *19*, 6272.
29. Lima C. H. S., Henriques M. G. M. O., Candea A. L. P., Lourenço M. C. S., Bezerra F. A. F. M., Kaiser C. R., de Souza M. V. *N. Med. Chem.* 2011, *7*, 245.
30. Ferreira M. L., Gonçalves R. S. B., Cardoso L. N. F., Kaiser C. R., Candea A. L. P., Henriques M. G. M. O., Lourenço M. C., Bezerra F. A. F. M., de Souza M. V. N. *Sci. World J.* 2010, *10*, 1347.
31. de Souza M. V. N., Pais K. C., Kaiser C. R., Peralta M. A., Ferreira M. L., Lourenço M. C. S. *Bioorg. Med. Chem.* 2009, *17*, 1474.
32. Vergara F. M. F., Lima C. H. S., Henriques M. G. M. O., Candea A. L. P., Lourenço M. C. S., Ferreira M. L., Kaiser C. R., de Souza M. V. N. *Eur. J. Med. Chem.* 2009, *44*, 4954.
33. Lourenço M. C., Ferreira M. L., de Souza M. V. N., Peralta M. A., Vasconcelos T. R. A., Henriques M. G. M. O. *Eur. J. Med. Chem.* 2008, *43*, 1344.

34. Pinheiro A. C., de Souza M. V. N., Lourenco M. C. S., da Costa C. F., Baddeley T. C., Low J. N., Wardell S. M. S. V., Wardell J. L. *J. Mol. Struct.* 2018, *1178*, 655.
35. Nogueira T. C. M., Cruz L. D., Lourenco M. C., de Souza M. V. N. *Lett. Drug. Des. Disc.* 2019, *16*, 792.
36. Correira N. R. L., Noguiera T. C. M., Pinheiro A. C., de Souza M. V. N., Wardell J. L., Wardell S. M. S. V. *Z. Kristallogr.* 2016, *231*, 271.
37. Bispo M. L. F., de Alcantara C. C., Wardell S. M. S. V., de Souza M. V. N., Wardell J. L. *Z. Kristallogr.* 2015, *230*, 519–530.
38. de Souza M. V. N., Noguiera T. C. M., Wardell S. M. S. V., Wardell J. L. *Z. Kristallogr*. 2014, *229*, 587.
39. Rodrigues F. A. R., Bomfim I. S., Cavalcanti B. C., Pessoa C. O., Wardell J. L., Wardell S. M. S.V., Pinheiro A. C., Kaiser C. R., Nogueira T. C. M., Low J. N., Gomes L. R., de Souza M. V. N. *Bioorg. Med. Chem. Lett.* 2014, *24*, 934.
40. Howie R. A., da Silva Lima C. H., Kaiser C. R., de Souza M. V. N., Wardell J. L., Wardell S. M. S. V. *Z. Kristallogr.* 2010, *225*, 158.
41. Bispo M. L.F., de Alcantara C. C., Wardell S. M. S. V., de Souza M. V. N., Wardell J. L. *Z. Kristallogr.* 2016, *231*, 21.
42. Ravish I., Raghav N. *Biochem. Anal. Biochem.* 2016, *5*, 1000253.
43. Kamal R., Kumar V., Bhardwaj V., Kumar V., Aneja K. R. *Med. Chem. Res.* 2015, *24*, 2551.
44. Kaplancıklı Z. A., Yurttas L., Turan-Zitouni G., Özdemir A., Göger G., Demirci F., Mohsen U. A. *Lett. Drug Des. Disc.* 2013, *11*, 76.
45. Pape V. F., Türk D., Szabó P., Wiese M., Enyedy E. A., Szakács G. *J. Inorg. Biochem.* 2015, *144*, 18.
46. Sharma A., Kumar V., Khare R., Gupta G. K., Beniwal V. *Med. Chem. Res.* 2015, *24*, 1830.
47. Tuberculosis. WHO. 2020, https://www.who.int/news-room/fact-sheets/detail/tuberculosis.
48. Chin K. L., Sarmiento M. E., Alvarez-Cabrera N., Norazmi M. N., Acosta A. *Eur. J. Clin. Microbiol. Inf.* 2020, *19*, 799.
49. Groom C. R., Bruno I. J., Lightfoot M. P., Ward S. C. *Acta Crystallogr.* 2016, *B72*, 171.
50. Franzblau S. G., Witzig R. S., McLaughlin J. C., Torres P., Madico G., Hernandez A., Degnan M. T., Cook M. B., Quenzer V. K., Ferguson R. M., Gilman R. H. *J. Clin. Microbiol.* 1998, *36*, 362.
51. Vanitha J. D., Paramasivan C. N. *Diagn. Microbiol. Infect. Dis.* 2004, *49*, 179.
52. Reis R. S., Neves I. Jr., Lourenço S. L. S., Fonseca L. S., Lourenço M. C. S. *J. Clin. Microbiol.* 2004, *42*, 2247.
53. CrysAlisPRO (version 1.171.39.9g); Agilent Technologies, Rigaku Oxford Diffraction: Yarnton, Oxfordshire (U.K.), 2015.
54. Sheldrick G. M. *Acta Crystallogr.* 2008, *A64*, 112.
55. Spek A. L. *Acta Crystallogr.* 2009, *D65*, 148.
56. Johnson C. K., Burnett M. N. Ortep-III (version 1.0.2), *Oak Ridge Thermal Ellipsoid Plot Program for Crystal Structure Illustrations*, Report ORNL-6895, Oak Ridge National Laboratory: Oak Ridge, TN (USA), 1996. Windows version: Farrugia L. J. *J. Appl. Crystallogr.* 1997, *30*, 565.
57. Mercury (version 3.9); Cambridge Crystallographic Data Centre: Cambridge (U. K.), 2019.
58. Shakdofa M. M. E., Shtaiwi M. H., Mosy N., Abdel-Rassel T. M. A. *Main Group Chem.* 2014, *13*, 187.
59. Narayana L. N., Sung-Ok B. *Res. J. Biotech.* 2017, *12*, 66.
60. Gupta S., Pal S., Barik A. K., Hazra A., Roy S., Mandal T. N., Peng S.-M., Lee G.-H., El Fallah M. S., Tercero J., Kar S. K. *Polyhedron* 2008, *27*, 2519.
61. Ray S., Konar S., Jana A., Das K., Dhara A., Chatterjee S., Kar S. K. *J. Mol. Struct.* 2014, *1058*, 213.
62. Vazquez-Garcia D., Fernandez A., Lopez-Torres M., Rodriguez A., Varela A., Pereira M. T., Vila J. M., Fernandez J. *J. Organometallics* 2011, *30*, 396.
63. Yuan J., Liu M.-J., Liu C.-M., Kou H.-Z. *Dalton Trans.* 2017, *46*, 16562.
64. Pradhan R., Banik M., Cordes D. B., Slawin A. M. Z., Saha N. C. *Inorg. Chim. Acta.* 2016, *442*, 70.
65. Ray S., Konar S., Jana A., Jana S., Patra A., Chatterjee S., Golen J. A., Rheingold A. L., Mandal S. S., Kar S. K. *Polyhedron* 2012, *33*, 82.
66. Enanga B., Ariyanayagam M. R., Stewart M. L., Barrett M. P. *Antimicrob. Agents Chemother.* 2003, *4*, 3368.
67. Hall B. S., Wilkinson S. R. *Antimicrob. Agents Chemother.* 2012, *56*, 115.
68. Carvalho S. A., Osorio L. F. B., Salomao K., de Castro S. L., Wardell S. M. S. V., Wardell J. L., da Silva E. F., Fraga C. A. M. *J. Heterocycl. Chem.* 2017, *54*, 3626.
69. Cardoso L. N. F., Bispo M. L. F., Kaiser C. R., Wardell J. L., Wardell S. M. S. V., Lourenço M. C. S., Bezerra F.A. F. M., Soares R. P. P., Rocha M. N., de Souza M. V. N. *Arch. Pharm. Chem. Life Sci.* 2014, *347*, 432.
70. Sander T., Freyss J., von Korff M., Rufener C. *J. Chem. Inf. Model.* 2015, *55*, 460.
71. http://hydra.vcp.monash.edu.au/modules/mod2/bondlen.html.
72. Bernstein J., Davis R. E., Shimoni L., Chang N.-L. *Angew. Chem. Int. Ed. Engl.* 1995, *34*, 1555.
73. Sankarganesh M., Raja J. D., Sakthikumar K., Solomon R. V., Rajesh J., Athimoolam S., Vijayakumar V. *Bioorg. Chem.* 2018, *81*, 144.
74. Gupta S., Pal S., Barik A. K., Roy S., Hazra A., Mandal T. N., Butcher R. J., Kar S. K. *Polyhedron* 2009, *28*, 711.
75. Amaral S. S., Campos P.T., dos Santos J. M., Fernandes L. S., Martins M. A. P., Bonacorso H. G., Zanatta N. *Open Crystallogr. J.* 2010, *3*, 59.
76. Le Fouler V., Chen Y., Gandon V., Bizet V., Salome C., Fessard T., Liu F., Houk K. N., Blanchard N. *J. Am. Chem. Soc.* 2019, *141*, 15901.
77. Shi J.-T., Gong Y.-L., Li J., Wang Y., Chen Y., Ding S., Liu J. *Chin. J. Struct. Chem.* 2019, *38*, 1530.
78. Gu W., Wu R., Qi S., Gu C., Si F., Chen Z. *Molecules* 2012, *17*, 4634.
79. Pejov L. *Chem. Phys. Lett.* 2001, *339*, 269.
80. Geng Y., Takatani T., Hohenstein E. G., Sherrill C. D. *J. Phys. Chem. A* 2010, *114*, 3576.
81. Gosling M. P., Pugliesi I., Cockett M. C. R. *Phys. Chem. Chem. Phys.* 2010, *12*, 132.
82. Fun H.-K., Loh W.-S., Nayak S. P. *Acta Crystallogr.* 2010, *E66*, o2467.
83. Dhara A., Guchhait N., Bhattacharya S. C. *J. Ind. Chem. Soc.* 2017, *94*, 781.
84. Lukov V. V., Tsaturyan A. A., Tupolova Y. P., Levchenkov S. I., Vlasenko V. G., Popov L. D., Pankov I. V., Poler J. C. *CCDC 1845762: Experimental Crystal Structure Determination*, 2019; https://doi.org/10.5517/ccdc.csd.cc1zynq9.
85. Jiang N., Zuo J., Wang H., Han M., Zhai X. *Acta Crystallogr.* 2012, *E68*, o1557.
86. Sarel S., Avramovici-Grisaru S., Cohen S. *Heterocycles* 1998, *49*, 393.

Supplementary Material: The online version of this article offers supplementary material (https://doi.org/10.1515/znb-2020-0108).